

Short Communication

Effect of *Ochrobactrum sp.* on the Corrosion Behavior of 10MnNiCrCu Steel in Simulated Marine Environment

Jie Sun¹, Xiaodong Zhao^{1, *}, Husong Rong¹, Shiyu Yang¹, Shuai Wang¹, Zhongyi An¹, Yan Li², Xinlei Qu³

¹ School of Ocean, Yantai University, Yantai 264005, China;

² Qingdao Branch of Naval Aeronautical Engineering Academy, Qingdao 266041, China;

³ Shandong Nanshan Aluminum Co., Ltd., Yantai 265706, China

*E-mail: danielxdzhao@aliyun.com

Received: 15 November 2019 / Accepted: 3 January 2020 / Published: 10 February 2020

In this research, the corrosion behavior of 10MnNiCrCu steel in simulated marine environment containing *Ochrobactrum sp.* was studied by open circuit potential(OCP), electrochemical impedance spectra(EIS), polarization curves and scanning electronic microscopy(SEM). The results showed that the *Ochrobactrum sp.* developed a biofilm on the steel surface during its exponential growth period, which slowed down the corrosion rate of the steel temporarily. In the growth stability period, the consumption of dissolved oxygen and uneven cover of biofilm resulted in the oxygen concentration difference on the surface of the steel, which aggravated the local corrosion.

Keywords: Microbiologically influenced corrosion (MIC); *Ochrobactrum*; Electrochemical method; SEM

1. INTRODUCTION

Microbiologically influenced corrosion (MIC) refers to the corrosion induced by the activities of microorganisms, or influenced by their metabolites on the change of physical and chemical properties of contact materials[1]. Microorganisms generally exist in the natural environment such as air, soil, water and so on, and biofilm usually occurs on the metal surface with the bacterial growth and reproduction. The internal environment of biofilm is totally different from the natural environment outside, thus the corrosion of metal might be accelerated or inhibited [2-9].

MIC reduces the service life of industrial equipment and civil facilities, especially for the shipbuilding and shipping industry. Up to now, most of the MIC studies have been emphasized on the influence of anaerobic bacteria represented by sulfate-reducing bacteria(SRB)[10-13], while MIC research related to aerobic bacteria such as *Ochrobactrum sp.*, *Bacillus sp.* and *Pseudomonas sp.* was

less involved[14-16]. However, there are a wide variety of microorganisms in natural environment, and their effects on corrosion mechanism or process of metal materials are different for different species[17].

The 10MnNiCrCu steel has been used in the shipbuilding industry because of its superior mechanical properties[18]. However, the corrosion of materials under the influence of various microorganisms will inevitably be involved in the marine ships due to their service environment. *Ochrobactrum sp.* is a kind of hydrophilic bacteria widely existing in natural environment such as water, soil and plants. In this study, a kind of *Ochrobactrum sp.* was isolated from the natural marine environment. By SEM and electrochemical methods such as EIS and polarization curves, the effect of the bacteria on the corrosion behavior of 10MnNiCrCu steel was studied. The corrosion mechanism was also discussed with introduction of biodiversity into MIC study.

2. EXPERIMENTAL SECTION

2.1 Material

The 10MnNiCrCu steel used in the experiment was supplied by a domestic shipyard. The elemental composition(wt%) was as follows: C($\leq 0.12\%$), Si(0.40-0.70%), P($\leq 0.015\%$), S($\leq 0.010\%$), Mn(0.70-1.10%), Ni(0.50-1.10%), Cr(0.60-0.90%), Cu(0.40-0.60%), Ti($\leq 0.020\%$) V($\leq 0.080\%$) and Fe balance. The samples were processed into two specifications. The samples used for electrochemical measurements were machined to sheet electrodes with an exposed surface of 10mm \times 10mm, and the rest was sealed with epoxy resin in a cylindrical cavity. A copper wire was soldered to each sample for electrochemical measurements. The samples used for morphology observation were 10mm \times 10mm \times 10mm cubes. Before the experiment, the surface of the sample was polished with 240 to 1200# sandpapers, then rinsed with distilled water and degreased with acetone. The samples were placed in a deoxygenation chamber and tested after UV disinfection for 30 minutes.

2.2 Bacteria and culture

The strain of *Ochrobactrum sp.* used in the experiment was isolated from the seawater near Laizhou Bay. The composition of the medium used was as follows: 10 g peptone , 3 g beef extract, 5 g sodium chloride in 1 L deionized water, and the pH value was adjusted with 1 mol·L⁻¹ NaOH(7.0 \pm 0.2). The medium was autoclaved at 121°C for 20 min. The bacterial solution was prepared by introducing the enriched bacteria into the sterile medium at a volume ratio of 1:10. The inoculated medium was used as the experimental system of bacteria and cultured in a constant temperature incubator (28°C). In addition, the same amount of sterile liquid medium was used as the sterile system for comparison.

2.3 Growth curve

The growth curve of *Ochrobactrum sp.* was determined by turbidimetry. The purified *Ochrobactrum sp.* was cultured in constant temperature incubator for 7 days. According to the pre-set time gradient, the absorbance at the wavelength of 600 nm was determined by UT-1810 ultraviolet

visible spectrophotometer, and the average value was determined three times as a characterization of the amount of bacteria in a certain period of time.

2.4 Electrochemical measurements

The electrochemical analysis was performed using a PARSTAT 2273 electrochemical workstation. A three-electrode system was adopted, the 10MnNiCrCu steel was used as working electrode, a platinum sheet ($10 \times 10 \times 0.1$ mm) used as the counter electrode, and a saturated calomel electrode (SCE) as the reference electrode. After the system was stable, the open circuit potential was measured, and the electrochemical impedance spectroscopy (EIS) was measured in the frequency range of 10^{-2} - 10^5 Hz at intervals of 1 day and the amplitude of the sinusoidal voltage signal was 10 mV. The data processing was carried out by a ZSimpWin software, and the structure of the equivalent circuit and the parameters of each element were analyzed. The polarization curve was tested and scanned on the 7th day of the experiment. The scanning rate was 0.5mV/s, the scanning range was ± 250 mV relative to the open circuit potential, and the data were analyzed by C-view software.

2.5 Corrosion morphology observation

The samples used for corrosion morphology observation were immersed in the above-mentioned bacterial culture and sterile culture system for 7 days. After the samples were taken out, washed with distilled water, degreased and dried with acetone, and sprayed with palladium, the corrosion morphology was observed under the scanning electron microscope.

3. RESULTS AND DISCUSSION

3.1 Growth curve

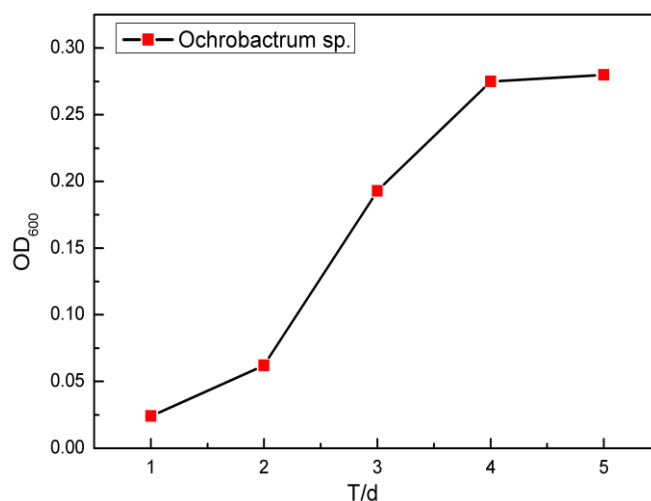


Figure 1. Growth curve of *Ochrobactrum sp.* with time in culture medium determined by turbidimetry

Fig. 1 shows the growth curve of *Ochrobactrum sp.* (in short, OS below) by turbidimetry. The results indicated that the growth of OS was relatively slow in the first two days. The reason was that

when the bacteria was inoculated into the culture system, the metabolic system needed to adapt to the new environment and produce synthase, coenzymes and other metabolic intermediates[19-20]. During 2-4d, the bacteria had entered an exponential phase of growth, and the amount of bacteria increased rapidly. From the 4th day to the end of the experiment, the cell proliferation reached a stable stage due to the consumption of nutrients or growth inhibited by the accumulation of metabolites, and the growth and death rate were balanced.

3.2 Open circuit potential(E_{ocp})

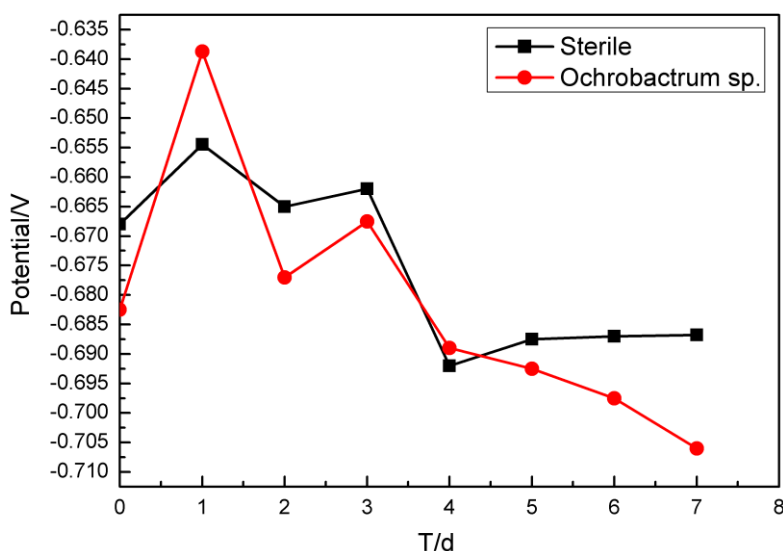


Figure 2. E_{ocp} of 10MnNiCrCu steel after immersion in sterile and OS-containing media over time

Fig. 2 showed the E_{ocp} (open circuit potential) of 10MnNiCrCu steel after immersion in OS and sterile media for different time. Generally, the variation of E_{ocp} in two systems were similar, there were negative shifts compared with the initial value. Moreover, the E_{ocp} in the OS system was significantly lower than that in the sterile system. The positive shift of E_{ocp} in the OS system for 1 day might be due to the formation of complexes by organic matter and metal cations on the metal surface[21]. Webster[22] also reported that the culture medium caused the positive shift of E_{ocp} by its temporary protective effect. During 4-7d, with the consumption of dissolved oxygen, the difference in oxygen concentration on the surface of the samples accelerated the corrosion, and there was a rapidly negative shift of the potential. In addition, *Ochrobactrum sp.* belonged to obligate aerobic and alkaline bacteria, which secreted alkaline substances by themselves[23]. The accumulation of these substances might lead to the aggravation of local corrosion. In sterile system, the variation of E_{ocp} was related to oxygen absorption corrosion and formation of corrosion product film.

3.3 EIS

Fig. 3 shows Nyquist and Bode diagrams of 10MnNiCrCu steels immersed in sterile and OS systems for 7 days. In the sterile system, the change of capacitance arc was not obvious in the first 2 days, which was consistent with the results of OCP. After immersion for 3 days, the value of impedance

modulus increased significantly. The corrosion product covering the sample surface might have a certain inhibiting effect on the corrosion of substrate. In the OS-containing system the capacitance arc increased gradually. As the *Ochrobactrum sp.* belonged to aerobic bacteria, the consumption of O_2 for its growth and reproduction inhibited the oxygen absorption corrosion in the system. The impedance modulus value was generally proportional to the corrosion resistance of the metal. In the OS-containing system, the value was obviously lower than that of the sterile system at the later stage (3d-7d) of immersion. The results showed that the corrosion of steel was increased in the presence of OS.

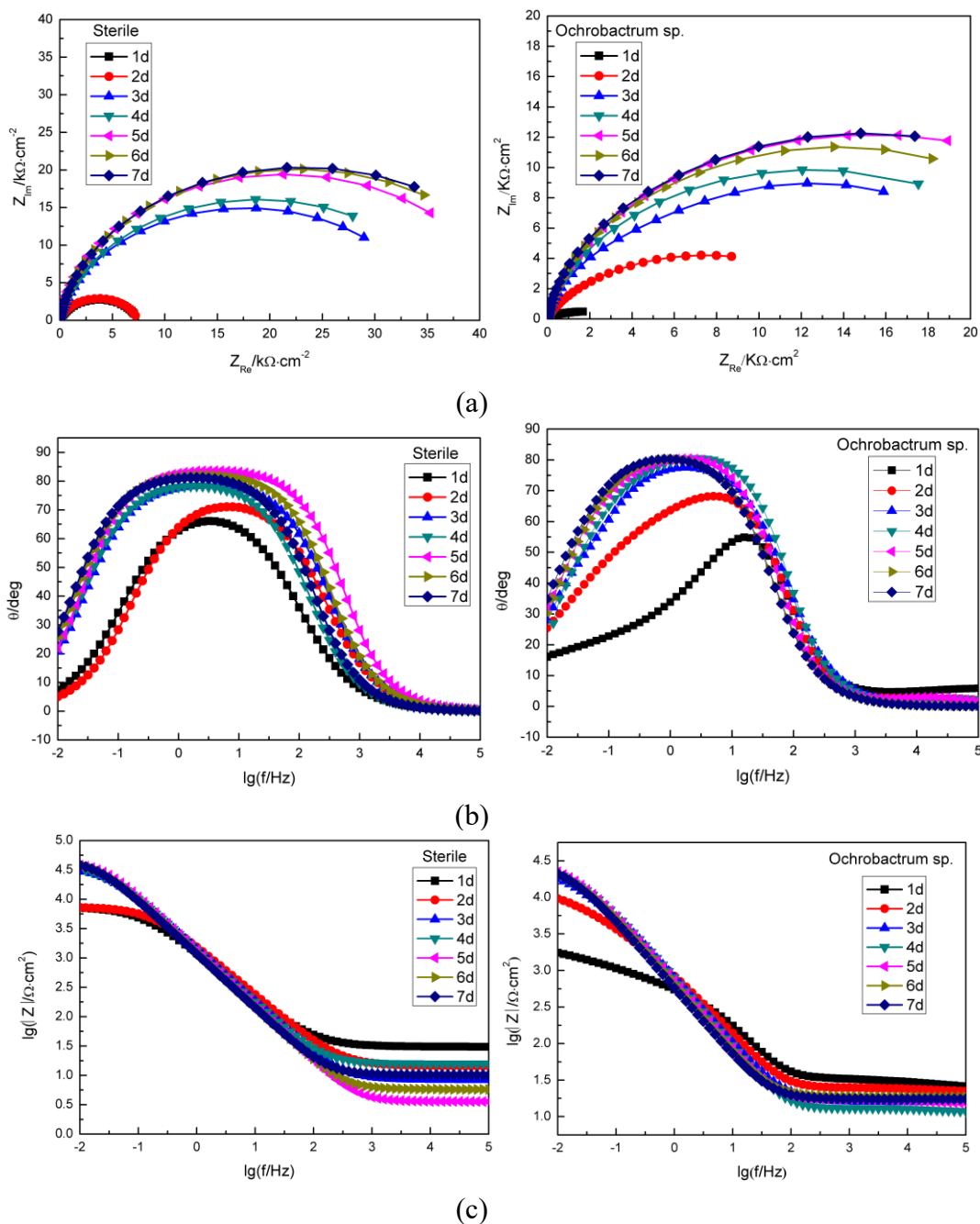


Figure 3. Nyquist and Bode diagrams of 10MnNiCrCu steel immersed in sterile and OS-containing media for 7d (a represents the Nyquist diagram, b represents the magnitude diagram, and c represents the phase angle diagram).

ZSimpWin software was used to fit the EIS diagram with the corresponding equivalent circuits, as shown in Fig. 4. The sterile system was represented by circuit(a) and the OS system was represented by circuit(b). R_s represents the solution resistance, R_b represents the protective film resistance on the electrode surface, R_{ct} represents the charge transfer resistance, Q_b represents the protective film capacitance, Q_{dl} represents the double layer capacitance, Q represents the constant phase component CPE(when $n = 1$, $CPE = C$, that is, the capacitance at this time is the ideal capacitance). The results of fitting parameters are listed in Table 1.

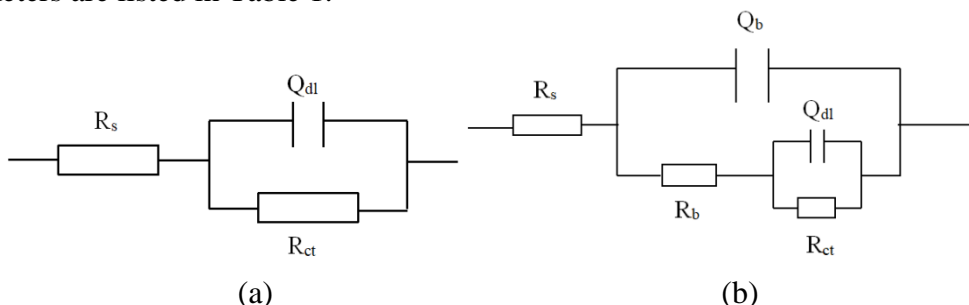


Figure 4. The equivalent circuit models used to fit the EIS experimental data for 10MnNiCrCu steel immersed in (a) sterile and (b) OS-containing media

Table 1. Parameter fitting values of each element in the equivalent circuit in Fig. 4.

System	T (d)	R_s ($\Omega \cdot \text{cm}^2$)	$Q_{dl} \times 10^{-4}$ ($\Omega^{-1} \cdot \text{cm}^{-2}$)	n_{dl}	R_{ct} ($\Omega \cdot \text{cm}^{-2}$)	$Q_b \times 10^{-4}$ ($\Omega^{-1} \cdot \text{cm}^{-2}$)	R_b ($\Omega \cdot \text{cm}^{-2}$)
Sterile	1	30.65	1.780	0.8105	7431		
	2	14.33	1.290	0.8435	7400		
	3	8.386	1.372	0.8920	35470		
	4	15.75	1.405	0.8953	37920		
	5	3.577	1.333	0.9398	42720		
	6	5.758	1.467	0.9251	45270		
	7	10.15	1.572	0.9207	46160		
OS	1	16.59	5.896	0.3226	3716	8.007	20.61
	2	21.35	8.148	0.5856	15660	2.515	4.41
	3	15.92	8.646	0.9029	8270	2.376	14290
	4	12.50	7.660	0.9300	6795	2.334	16600
	5	14.95	1.579	0.7122	31820	1.101	2.692
	6	18.81	11.78	0.9286	5145	2.810	21230
	7	17.38	15.33	0.9265	5440	3.151	23290

According to the data in Tab.1, as the factor n was an index of surface roughness[24], in the bacteria-containing system, basically n_{dl} and Q_{dl} increased at first and then decreased, subsequently increased, revealing that the electrode was in a adsorption state and a protective film developed gradually on the surface of the steel. In Fig. 5, the R_{ct} value increased slowly in sterile

medium, indicating that the corrosion rate of steel decreased gradually. In the bacteria-containing system, R_{ct} basically increased first and began to decrease in the later stage of the experiment, illustrating that the biofilm formed on the surface of steel had a certain protective effect in the early stage of immersion, and later with the destruction of the film, the corrosion rate increased.

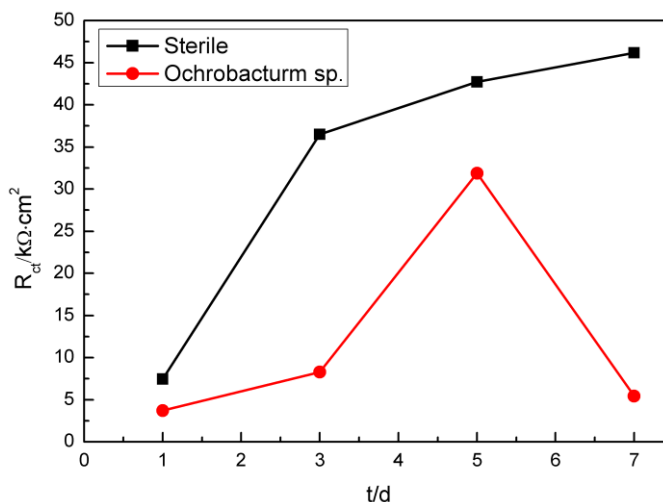


Figure 5. Variation of R_{ct} value over time for 10MnNiCrCu steel immersed in sterile and OS-containing system

3.4 Polarization curve

Fig. 6 shows the polarization curves of 10MnNiCrCu steel after immersion in sterile and OS-containing system for 7d. Tafel curves was fitted by C-view software, and the corresponding electrochemical parameters were obtained, as shown in Tab. 2.

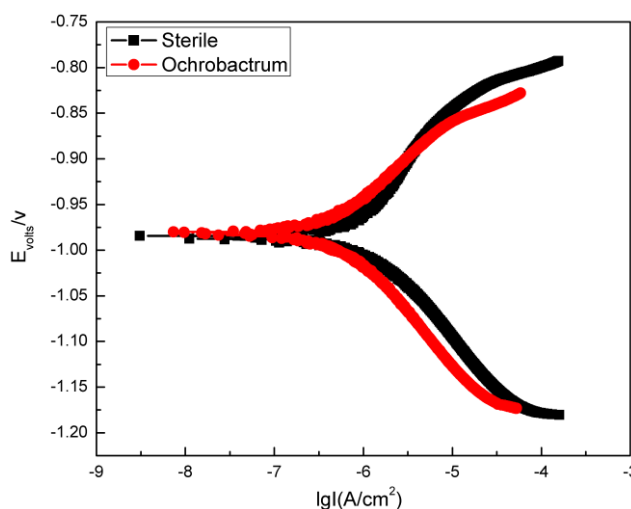


Figure 6. Polarization curves of 10MnNiCrCu steel after immersed in sterile and OS-containing media for 7d

According to Fig. 7 and Tab. 2, there were only slight difference of the corrosion current density (I_{corr}) and corrosion potential (E_{corr}) between the 10MnNiCrCu steels after immersion in two media. In the bacterial system, the corrosion current density was slightly higher than that of the sterile system, indicating that oxygen concentration cell formed between the biofilm and the uncovered substrate on the outer layer of the steel surface accelerated the localized corrosion[25-26].

In addition, it showed that the corrosion potential in the bacterial system was slightly higher than that in the sterile system(4mV), indicating that on the 7th day the corrosion tendency of 10MnNiCrCu steel in the OS-containing system was similar to that in the sterile system.

Table 2. Fitting values of polarization curves of 10MnNiCrCu steel after immersed in sterile and OS-containing media for 7d

System	E_{corr} (V)	I_{corr} ($\mu\text{A}/\text{cm}^2$)	B_a (mV/dec)	B_c (mV/dec)
Sterile	-0.984	1.086	158	113
OS	-0.980	1.126	146	163

3.5 Surface morphology analysis with SEM

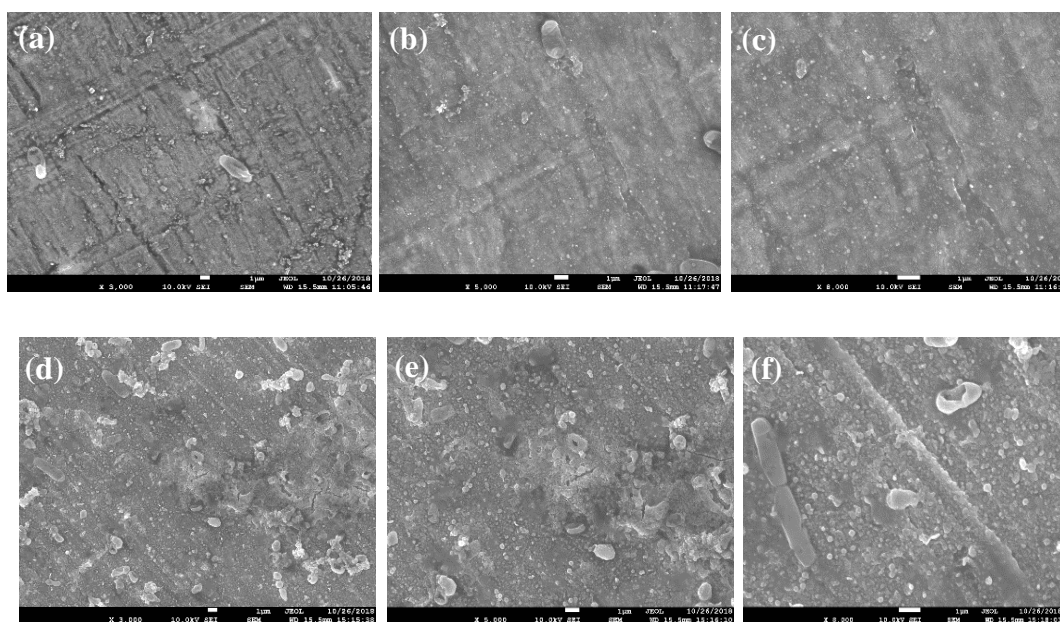


Figure 7. SEM images with different magnifications of surface morphology of 10MnNiCrCu steel after immersed in (a), (b), (c) sterile and (d), (e), (f) OS media for 7d

Fig. 7 shows the surface morphology of 10MnNiCrCu steel after 7d immersion in sterile and OS system at different magnification by SEM. It showed that after immersion, the surface was smooth and uniform with few contaminants in the sterile system, while in the OS-containing media, a layer of corrosion products developed on the surface of the steel. The film was uneven and there were many cracks and holes, which provided conditions for pitting corrosion and the formation of micro cells.

3.6 Discussion

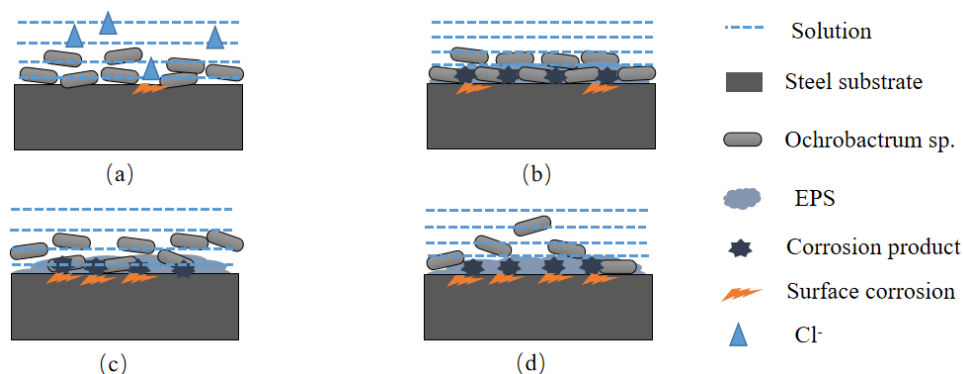


Figure 8. Schematic diagram of the effect of OS on the corrosion process of 10MnNiCrCu steel

Nardy[27] reviewed the main bacteria responsible for MIC, including sulfate-reducing bacteria (SRB), sulfur oxidizing bacteria, iron oxidizers, iron reducers, manganese oxidizers and microbes that secrete organic acids and produce extracellular polymeric substances (EPS). In the presence of bacteria, such as OS, the metabolites and EPS adsorbed on the metal surface will mostly accelerate or inhibit the metal corrosion. In a biofilm the interactions between different species may induce a cascade of biochemical reactions in the oxic and anoxic parts of the biofilm and aggravate corrosion[28]. Although the complexation reaction between the metabolites of OS and steel is not clearly known yet, *Ochrobactrum sp.* is found to be able to bind and accumulate metal ions in the form of superficial mucilage layer contained in EPS[29-32], and the corrosion process of the steel could be discussed based on the results of the above work.

In marine environment, Cl^- and oxygen content are important factors that affect the corrosion of materials. At the initial stage of immersion, the bacteria propagated in large numbers and adsorbed on the surface of steel. During this process, the dissolved oxygen near the steel surface was consumed continuously and a barrier was formed on the surface of the steel to prevent the diffusion of Cl^- due to the adsorption effect of the bacteria. The corrosion of steel in this stage was inhibited compared with that in sterile environment(Fig. 8 (a)). After a period of immersion, the bacteria and EPS further developed a biofilm, which accelerated the steel corrosion(Fig. 8 (b)). In the later stage of immersion (Fig. 8 (c)), as the adsorption effect of the bacteria and EPS became weak, and the oxygen content near the steel surface kept decreasing, the bacteria spread to the high oxygen area or declined due to the insufficient nutrient (Fig. 8 (d)). At the same time, due to the uneven biofilm, oxygen concentration cell was easy to be formed on the steel surface, which accelerated the corrosion process.

4. CONCLUSION

The purpose of this experiment is to understand the influence of *Ochrobacturm sp.* on the corrosion of 10MnNiCrCu steel in 3.5% NaCl solution. By analysis of a series of electrochemical and microscopic results, the following conclusions can be drawn:

(1) A layer of biofilm of *Ochrobacturm sp.* developed on the surface of 10MnNiCrCu steel at the early stage of the growth, which had a positive effect on temporary inhibition of the corrosion of 10MnNiCrCu steel.

(2) The week adhesion of *Ochrobacturm sp.* led to the separation of biofilm from the surface of 10MnNiCrCu steel in the later stage of the experiment, and then the oxygen concentration cell due to the uneven corrosion product film accelerated the corrosion process.

ACKNOWLEDGMENTS

This research was supported by Scientific Research Foundation of Yantai University and the Research Project of Department of Education of Shandong Province of China under Grant No.J17KA220 are also gratefully acknowledged.

References

1. H. Liu and H. F. Liu, *J. Chin. Soc. Corros. Prot.*, 37(2017)195.
2. H. W. Liu, T. Y. Gu, M. Asif, G. A. Zhang and H. F. Liu, *Corros. Sci.*, 114(2017)102.
3. J. Yang, J. Shao, L. Wu, Y. Li, X. D. Zhao, S. Wang, D. Y. Sun and J. Sun, *Int. J. Electrochem. Sci.*, 14 (2019) 9193.
4. X. D. Zhao, K. F. Chen J. Yang, G. F. Xi, H. T. Tian and Q. G. Chen, *Int. J. Electrochem. Sci.*, 14 (2019) 875.
5. X. D. Zhao, K. F. Chen J. Yang, G. F. Xi, H. T. Tian and Q. G. Chen, *Int. J. Electrochem. Sci.*, 14 (2019) 886.
6. H. F. Liu, L. Huang T. Liu and Y. L. Hu, *J. Chin. Soc. Corros. Prot.*, 29(2009)154.
7. Z. H. Dong, T. Liu and H. F. Liu, *Biofouling*, 27(2011)487.
8. R. Jia, D. Yang and J. Xu, *Corros. Sci.*, 127(2017)1.
9. A. Kogo, S. J. Payne and R. C. Andrews, *Environ. Eng. Sci.*, 34(2017)711.
10. D. Yang, Y. Lei and J. Xie, *Mater. Technol.*, 34(2019)444.
11. P. Zhang, D. Xu and Y. Li, *Bioelectrochemistry*, 101(2015)14.
12. Z. H. Dong, W. Shi and H. M. Ruan, *Corros. Sci.*, 53(2011)2978.
13. Z. Shahryari, K. Gheisari and H. Motamedi, *Mater. Chem. Phys.*, 236(2019)121799.
14. A. Reyes, M. V. Letelier, R. D. Iglesia, B. Gonza' lez and G. Lagos, *Int. Biodeterior. Biodegrad.*, 61(2008)135.
15. M. B. Valcarce, S. R. De Sánchez and M. Vazquez, *Corros. Sci.*, 47(2005)795.
16. J. E. G. González, A. F. J. H. Santana and J. C. Mirza-Rosca, *Corros. Sci.*, 40(1998)2141.
17. Y. Li, D. Xu and C. Chen, *J. Mater. Sci. Technol.*, 34(2018)1713.
18. D. Fuente, I. Díaz and J. Simancas, *Corros. Sci.*, 53(2011)604.
19. S. Ray and V. C. Kalia, *Bioresour. Technol.*, 224(2017)743.
20. Y. Gu, X. Q. Lv, Y. F. Liu, J. H. Li, G. C. Du, J. Chen, L. Rodrigo and L. Liu, *Metab. Eng.*, 51(2019)59.
21. A. Iversen, *Br. Corros. J.*, 36(2013)284.
22. B. J. Webster and R. C. Newman, *Producing rapid sulfate-reducing bacteria (SRB)-Influenced corrosion in the laboratory*. West Conshohocken, PA: ASTM International, 1994.
23. J. Guo, X. Liu and L. Sun, *J. Environ. Eng.*, 1(2007)136.
24. K. Chai, Q. Luo and J. Wu, *J. Chin. Soc. Corros. Prot.*, 33(2013)481.
25. A. A. Oskuie, T. Shahrabi, A. Shahriari and E. Saebnoori, *Corros. Sci.*, 61(2012)111.
26. S. Ye, M. Moradi, Z. Song, F. Q. Hu, C. H. Sun and J. P. Long, *J. Chin. Soc. Corros. Prot.*, 38(2018)174.
27. K. Nardy and J. A. van Veen, *ISME J.*, 9(2015)542.

28. H. A. Videla and L. K. Herrera, *Int. Biodeterior. and Biodegrad.*, 63(2009)896.
29. R. A. Manrique, P. I. Magana, V. Lopez and R. Guzman, *Curr. Microbiol.*, 41(2000)232.
30. N. Ahalya, T. V. Ramachandra and R. D. Kanamadi, *Res. J. Chem. Environ.*, 7(2003)71.
31. O. Guven, O. Tansel, C. Nur, I. Rahim and C. Tamer, *Bioresour. Technol.*, 90(2003)71.
32. N. H. N. Raikhan, M. S. A. N. Nadila and A. R. K. Izwan, *Int. J. Conserv. Sci.*, 9(2018)439

© 2020 The Authors. Published by ESG (www.electrochemsci.org). This article is an open access article distributed under the terms and conditions of the Creative Commons Attribution license (<http://creativecommons.org/licenses/by/4.0/>).